Observation of large tunneling-conductance variations in direct mapping of the energy gap of single-crystal $Bi_2Sr_2CaCu_2O_{8-x}$

A. Chang, Zhao Y. Rong, Yu. M. Ivanchenko, Farun Lu, and E. L. Wolf
Department of Physics, Polytechnic University, Brooklyn, New York 11201
(Received 1 May 1992)

The tunneling conductance $G(V,x,y)$ is mapped with 5 Å resolution on cleaved a-b planes of $Bi_2Sr_2CaCu_2O_{8-x}$ crystals ($T_c=90$ K) using scanning (vacuum) tunneling spectroscopy at 4.2 K. A strong, spatially varying $G(V,x,y)$, evidently arising from a superconducting gap Δ_c, is observed on the a-b plane. A more highly peaked $G(V)$ with reduced peak spacing is seen near (~ 50 Å) specific sites, and over broader areas. It is suggested that the striking variations in $G(V,x,y)$ probably indicate local variations in BiO-layer metallicity, revealing an internal superconducting proximity effect between BiO and CuO_2 layers.

The origin of superconductivity in the high-T_c cuprates (HTS) remains obscure and of great interest. Measurement of the electronic spectrum [density of states (DOS)] of the HTS, probably its most revealing property, is very difficult. The best methods, photoemission spectroscopy (PES) and tunneling $dI/dV=G(V)$ [vacuum tunneling spectroscopy (VTS)], require surface perfection on an atomic scale because of their short ≤ 10 Å sampling depths, coupled with the small superconducting coherence lengths, e.g., $\xi_c \sim 1$ Å, $\xi_{a,b} \sim 24$ Å (Ref. 1) in $Bi_2Sr_2CaCu_2O_{8-x}$ (2:2:1:2). Rapid experimental progress has recently been made in the layered compound 2:2:1:2, by exploiting its ease of cleavage and the inert nature of the exposed BiO layer. Quite similar and interestingly anomalous DOS spectra, believed to be characteristic of such HTS, have recently been provided by PES (Refs. 2–4) on UHV-cleaved 2:2:1:2, and, in less detail, by VTS (Refs. 5–7) on 2:2:1:2 crystals air cleaved at 300 K, rapidly cooled to 4.2 K for measurement. These remarkably similar spectra provide confidence that the PES and VTS methods both measure the electronic spectrum of the HTS as one would expect. These results open questions, in 2:2:1:2, particularly, on the role of metallicity and the origin of superconductivity in the BiO layer.

Superconductivity in 2:2:1:2 exists over a range of O stoichiometry, x, corresponding to a variation in the Hall-carrier concentration n, varying from $3.1\times10^{21}/\text{cm}^3$ ($T_c=91$ K) to $4.6\ 10^{21}/\text{cm}^3$ (77 K).[8] Oxygen-annealed 2:2:1:2 ($77<T_c<90$ K) is composed of 15.4 Å half-cells along the c axis, each with two superconducting CuO_2 sheets (S) at the center, sandwiched in turn by two insulating SrO sheets (I) and by two metallic BiO sheets (N), whose inert outer surfaces are revealed by cleaving: such fully metallized half-cells are of the form N-I-S/S-I-N. Here N suggests an inherently normal layer which can be induced superconducting by the proximity effect (SPE). In fact, SPE is the basis of a theoretical description of the cuprates[9] which emphasizes that DOS spectra are specific to each layer of the structure. However, *nonmetallic* BiO sheets [$N_{\text{BiO}}(0)\approx 0$] are indicated in (91 K) vacuum or argon annealed (and possibly as-grown 90 K) samples by PES (Ref. 2) and by specific heat C_v.[10] The $C_v(T)$ then shows greater fluctuation superconductivity above T_c, consistent with a more two-dimensional structure, which would result from the absence of the metallic N layers. The observed T_c lowering (14%) in the fully metallized N-I-S/S-I-N case would naturally result if the (verified[2–4]) superconductivity in N [for $N_{\text{BiO}}(0)>0$] arises by SPE.

The *local* tunneling DOS, $dI/dV=G(V,x,y)$, and the gap amplitude Δ are particularly susceptible to spatial variation in HTS (1) because of the importance of defects and local stoichiometry variations[11] in allowing these internally noncommensurate crystals to form over a range of compositions x and (2) because of the reduced averaging of such fluctuations as a consequence of small ξ. Hence one expects a local DOS measurement, scanning (vacuum) tunneling spectroscopy (STS), to reveal, in spatial dependence, portions of the range of behavior expected (above) with differing n, T_c, and Δ for varying stoichiometry, x. High-resolution STS maps of $G(V,x,y)$ and $\Delta(x,y)$ are of great interest, extending, to high-resolution mapping, the methods and interpretation established by VTS,[5–7] thus far limited to selected spectra, not correlated with location.

We present, for the a-b plane of $Bi_2Sr_2CaCu_2O_{8-x}$ (2:2:1:2), results on $G(V,x,y)$ mapping (with the requisite resolution $<\xi_{a,b}$; here 5 Å).[12] Note that atomic resolution is not required here, although it is well known[5–7] that this is not precluded by the brief air exposure. We find local variations in $G(V,x,y)$, and, making use of the simultaneously obtained topographs $z(x,y)$, find some correlation with local variations in $N_{\text{BiO}}(0,x,y)$, closely related to the metallicity of the BiO surface. Modeling suggests that the intriguing "highly peaked" electronic spectra that we find probably arise by an internal SPE between the S and N layers in fully metallized regions.

The apparent surface height z in constant current mode STM varies with $N_{\text{BiO}}(0,x,y)$ even for a perfectly flat geometry, since $I=\text{const}=N_{\text{BiO}}(0,x,y)\times\exp[-\phi^{1/2}z(x,y)]$. If we take ϕ as constant[13] 0.5 eV, as reported,[7] roughly consistent with our estimate, a non-

structural $z'-z=\Delta z=5$ Å implies an increased $N'/N\approx 40$, which could metallize the surface. Such "electronic" z peaks, already reported on the a-b surface of 2:2:1:2,[7,13] seem to contribute to our $z(x,y)$ data.

We have grown large single crystals in the $T_c=90$ K 2:2:1:2 phase, from BiO-rich melts,[14] characterized by resistivity, x-ray diffraction, and χ_{ac} as described elsewhere.[15] Figures 1(a) and 1(d) show $z(x,y)$ on the same 500×500 Å^2 of 2:2:1:2 at 4.2 K using a Pt-Ir tip. The crystal was cleaved in air and rapidly (15 min.) mounted and immersed in ^{4}He for STM measurement. This procedure, as used in VTS studies of 2:2:1:2,[5-7] provides a high-quality surface, which is made possible by the inert nature of the BiO layer. (In a conventional tunneling study[15] of the same 2:2:1:2 crystals, Pb crossing layers were applied after five days air exposure, and the junctions clearly reveal gap spectra.) The vibration levels in our cryogenic STM preclude resolving the individual Bi atoms. Bi atoms are seen using a more stable STM [Fig. 1(c)], which provides assurance that regions of atomically flat a-b BiO surfaces result from our cleaving process. The 100×100 raster scan (Fig. 1) measured $z(x,y)$ and $I(V)$ at 5 Å intervals, for a total of 10^4 points. The range of the gray scale [Fig. 1(a)] is ≈ 40 Å; z falls an additional ≈ 100 Å in a highly stepped region at $x>400$ Å. Similar stepped regions were reported by Kirk *et al.*;[16] reasons for depressed superconductivity in such regions have been given by Komeda *et al.*[17] To the left of Fig. 1(a), seen more clearly in Fig. 1(d), are two a-b plane plateaus separated by an apparent grain boundary near $y=350$ Å extending from $x=0$ to $x\approx 400$ Å.[18] The lack of atomic resolution in Figs. 1(a) and 1(b) is attributed to the larger scale of the region and larger vibrations in our cryogenic STM. The overall roughness of the upper and lower plateau regions is on the order of 5 Å, which we attribute primarily to local changes in $N_{\mathrm{BiO}}(0,x,y)$ (above),[7,19] and to unresolved superstructure. Note that even in Fig. 1(c), with a very restricted 15 Å range, there is some variation in z (brightness), presumably due to electronic effects.[7,19] However, we cannot rule out that some of the variation in z in the plateaus of Figs. 1(a) and 1(d) comes from a spatial variation in ϕ. Our main contributions are greatly

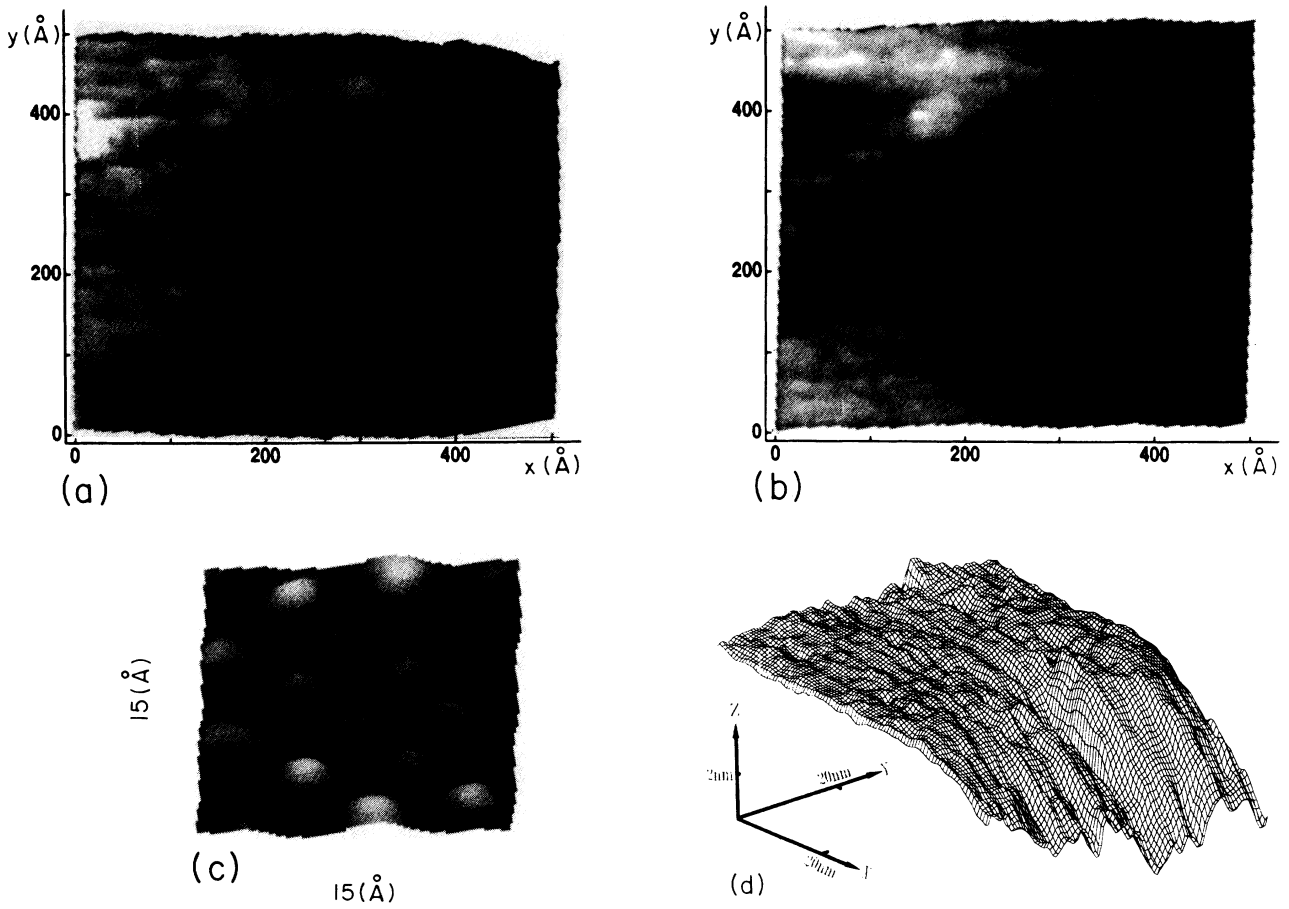

FIG. 1. (a) Topograph at 4.2 K of 500×500 Å^2 region at 5 Å spacing; 1 nA at 200 mV tip bias. Gray scale range [$z(x,y)$ variation] is 40 Å; in a highly stepped region (right), z falls a further ≈ 100 Å, off scale. (b) Gray scale image of maximum $G_{\mathrm{Peak}}(x,y)/G(168$ mV) of $G(V)$, $-168<V<168$ mV (tip bias), acquired in 10^4 pixels. White areas exhibit $G_{\mathrm{Peak}}/G(168$ mV) up to ~ 1.9. (c) Topograph of 15×15 Å^2 square of similar BSCCO crystal *in situ* cleaved and imaged using a more stable STM at 1.2×10^{-9} Torr, using etched Pt-Ir tip at -290 mV and 1.2 nA current. (d) Perspective view of the same data as in (a), calibration shown, which more clearly reveals details near the joining of the two plateau regions, $0<x<30$ Å, 350Å$<y<400$ Å.

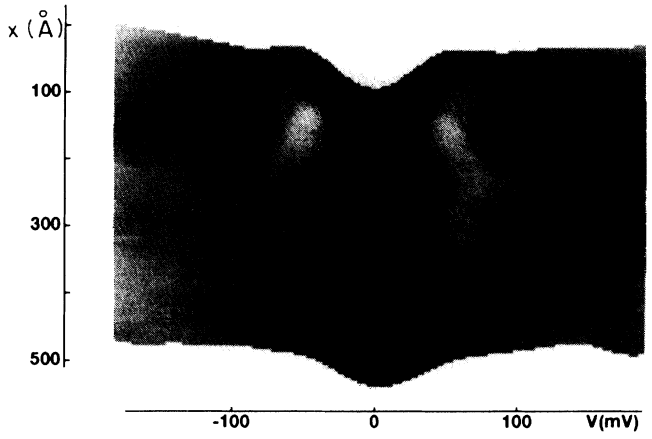

FIG. 2. Local variation of $G(v,x,y)/G(168\text{ mV})_{av}$ (gray scale range 0.12–1.36). Curves taken at 5-Å intervals for $0<x<500$ Å (top to bottom), averaging $G(V)$ over $375<y<400$ Å (six rows).

improved (5 Å) resolution in mapping $G(V,x,y)$ and energy gap, quantities not expected to vary on a scale less than $\xi_{a,b}\approx 24$ Å, and the resulting evidence for an internal proximity effect.

At each pixel in Figs. 1(a), 1(b), and 1(d), 16 $I(V)$ scans of 100 points, $-200<V<200$ mV, were averaged, and the 10^4 distinct $dI(V)/dV$ curves obtained from coefficients of least-squares fit polynomials. Figure 1(b) maps the peak value $G_{peak}(x,y)/G(168\text{ mV})$,[20] occurring at V_{peak} near $V=\Delta/e$. Generally, a strongly varying $G(V)$—as expected for superconductivity, and similar to prior PES (Refs. 2–4) and VTS (Refs. 5–7) results identified as the superconducting DOS—appears on the plateaus shown in Figs. 1(a), 1(b), and 1(d), but disappears in the highly stepped region $x>375$ Å, and in the narrow localized regions near the left end of the grain boundary, $0\le x\le 30$ Å and $350\le y\le 400$ Å, where steps may also exist. For $x>375$ Å and for $0\le 30$ Å and $350\le y\le 400$ Å, the $G(V)$ spectra typically show a minimum (pseudogap) at $V=0$, and in some regions a V shape, both resulting in "valleys" or dark regions in Fig. 1(b). Interesting regions of especially large $G_{Peak}/G(168\text{ mV})$ ("highly peaked" spectra) are seen as bright portions to the upper left corner of Fig. 1(b).

Remarkable local variations in $G(V,x,y)$ are present in our complete data set, notably near local maxima in $G_{Peak}(x,y)$ [bright spots in Fig. 1(b)]. Figure 2, a gray-scale representation of 100 distinct $G(V)$ curves [$\delta x=5$ Å, $0<x<500$ Å, averaging $G(V)$ over $375<y<400$ Å^2 (six rows)] reveals "highly peaked" $G(V)$ in an ≈ 100 Å range near $x=165$ Å. Here the peaks in $G(V)$ close and heighten, each by about 20%. From the parameter summary in Fig. 3, we see that the "highly peaked" $G(V)$ correlates a maximum of $G_{Peak}(x,y)$ and minimum in $V_{Peak}(x,y)$ with a maximum of z at $x=175$ Å. This apparent 8-Å z peak, similar to those seen in Ref. 7, is higher and broader than expected from pure topography. Such variations are not present in the lower plateau where bright regions in the $G_{Peak}(x,y)$ gray scale do not occur. We interpret this 8-Å apparent peak of z, in a region plausibly geometrically flat (and assuming a constant work function), as a local increase in $N_{BiO}(0,x,y)$, promoting BiO metallicity, as discussed above.

While the "highly peaked" DOS is localized on a scale of 50 Å in Fig. 2, it is also observed over broader regions: the bright areas in Fig. 1(b). For example, Fig. 4 shows $G(V)$ curves from $y=430$ Å, $100<x<200$ Å^2, which are similar to the "peaked" curves in Figs. 2 and 3. These spectra [see also Fig. 5(a)] are typical of $G(V)$ in the bright regions in the upper left in Fig. 1(b), and appear to correlate in many cases with locally elevated apparent topography [brighter regions in Fig. 1(a)]. Such correlation is not expected where the topography sharply varies, e.g., near the prominence [best seen in Fig. 1(d)] at the lower left edge of the upper plateau ($0=x\le 30$ Å, $y\approx 400$ Å),

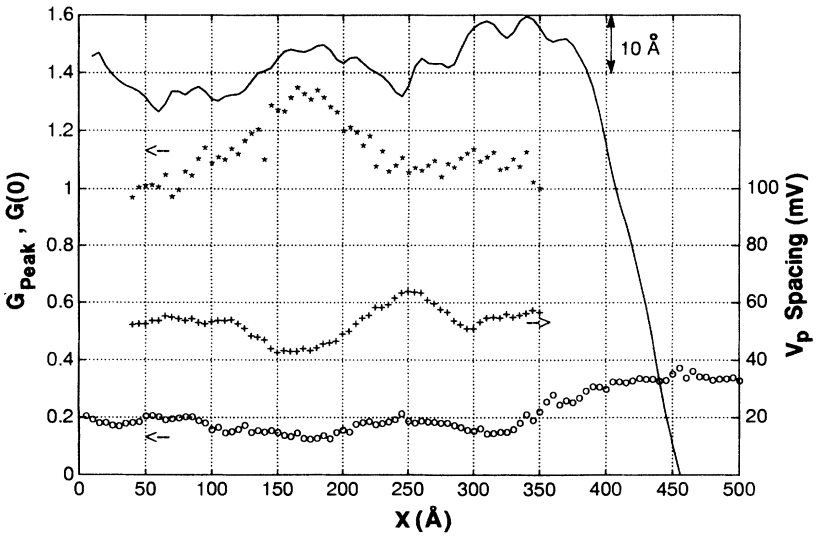

FIG. 3. Comparison of x variation, $0<x<500$ Å, of topographic and spectral features averaged over $375<y<400$ Å (six rows); see Fig. 2. Solid curve is $z(x)$ topography, 10 Å per division. $z(x)$ shows a maximum near $x=170$ Å (possibly of electronic origin); asterisks show normalized (Ref. 20) G_{Peak}, about 30% increased in this region, while the peak position $V_p(+)$ is reduced. The value of normalized $G(0)$ (○) increases in the highly stepped region $x>375$ Å.

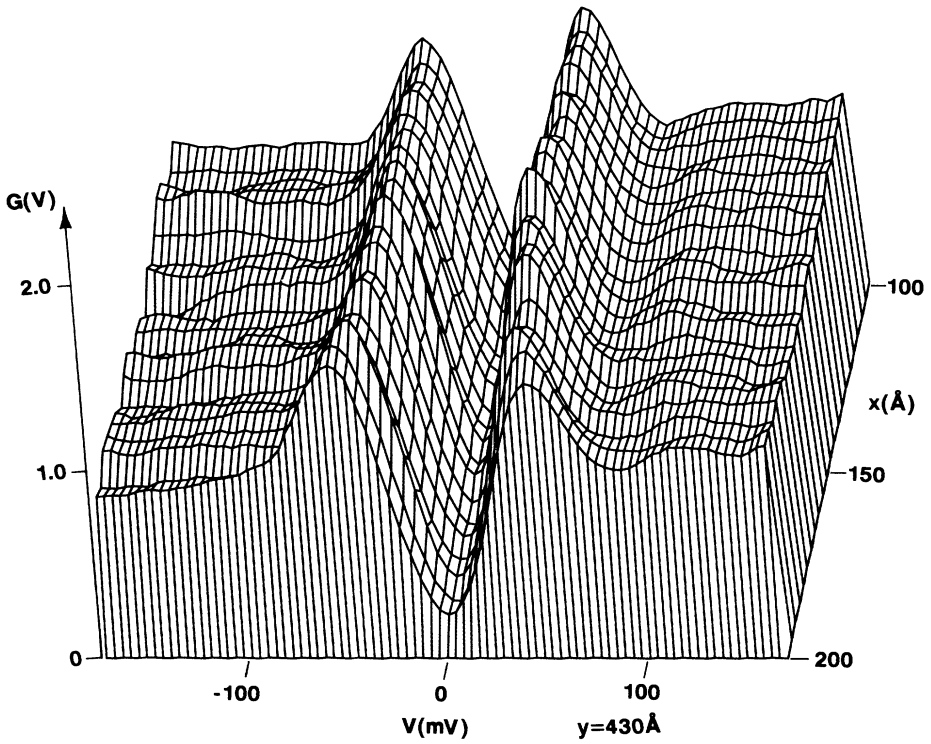

FIG. 4. $G(V,x,y)$ for $y=430$ Å, $100<x<200$ Å. These curves resemble in shape those near $x=170$ Å, $y=387$ Å (see Figs. 2 and 3).

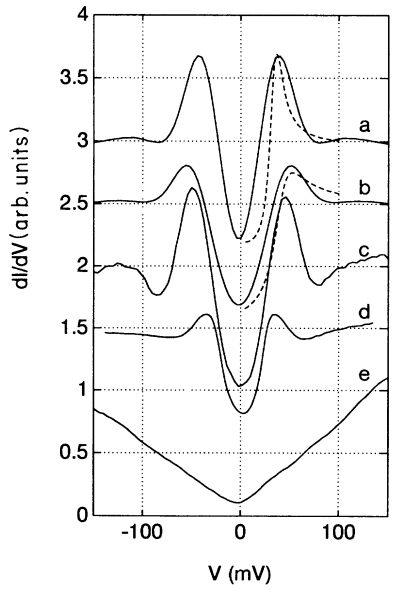

FIG. 5. Comparison of $G(V)$ obtained on BSCCO crystals at 4.2 K by c-direction tunneling. Curves a–e are normalized by the mean of the end-point values [corresponding to 1 nA in curves a, b, and e; 1 μA for curve c] and are displaced vertically in increments of 0.5. Curve a (solid) is the average of $G(V,x,y)$ for the 21 curves in Fig. 4: $y=430$ Å, $100<x<200$ Å. The even part of $G(V)$ is shown to facilitate comparison with the model (see the text) shown as dashes. b (solid) is the even part of $G(V,x,y)$ averaged over 500 points, $0<x<125$ Å, $0<y<100$ Å. Dashes are the model; see the text. c is a single curve obtained in a separate run in which the tip penetrated the sample; this curve was obtained as the tip was withdrawn. d is obtained in conventional tunneling from a Pb film (Ref. 15); e is from the highly stepped region in Fig. 1: $G(V,x,y)$ $y=305$ Å, averaging $455<x<500$ Å.

nor in highly stepped regions ($x>350$ Å; possibly for $0\leq x\leq 30$ Å, $y\approx 400$ and 350 Å) with sharp jumps in $z(x,y)$, for such regions seem to have a V-shaped nonsuperconducting $G(V)$, i.e., a dark region in Fig. 1(b). Note that a sharp jump in $z(y)$ occurs just below (and possibly just above) the prominence ($0\leq x\leq 30$ Å, $y\approx 400$ Å) in Fig. 1(d). [These features are obscured in Fig. 1(a) because of gray-scale saturation and x,y averaging.] These jumps may account for the disparity of the localized dark (bright) regions in Fig. 1(b) [Fig. 1(a)] at the corresponding location. In the less bright portions of the region $y>350$ Å in Fig. 1(b), the $G(V)$ resemble those in the lower plateau,[18] e.g., in the 100×125 Å^2 region at $x=0,y=0$. We believe that spatial variation in $G(V,x,y)$ most noticeable in the upper plateau certainly reflects local variations in the superconductivity at the surface. It is likely that the latter reflects variations in the local stoichiometry,[21] and particularly variations in the surface-Fermi-level DOS, $N_{\mathrm{BiO}}(0,x,y)$, rather than different crystalline orientations.[6]

Typical STS $G(V)$ spectra are shown in Fig. 5 (solid curves). (We discuss below the dashed curves, based on an internal SPE model.) Curve a (solid), the average of the 21 curves in Fig. 4, is characteristic of the "highly peaked" spectra. Curve b (solid), obtained from a 100×125 Å^2 region at $x=0,y=0$, is also seen in regions of the upper plateau. We identify curves of type a (b) with regions having metallic (nonmetallic) BiO layers. Figure 5(c) is $G(V)$ obtained in a separate run under point contact conditions, with a current level of 10^{-6} Å; d, with reduced V_{peak} values, is obtained with a Pb-I-BSCCO planar junction.[15] The linear $G(V)$ (e) is seen in portions of the highly stepped region and small regions of the grain boundary; a pseudogap-type spectrum is also seen, e.g., at $x=500$ Å in Fig. 2.

Discussion

The upper curves in Figs. 5(a) and 5(b) are quite similar to the photoemission electronic spectra of HTS.[2–7] In particular, curve *a* strikingly resembles the PES of Ref. 4. In detailed comparison of the present STS (curve *a* of Fig. 5) to the PES curve (Fig. 1 of Ref. 4) we find for STS (PES) normalized peak heights 1.67 (1.63), peak positions 39 mV (37.3 mV), width at unit height 45 mV (35 mV), and minimum positions 77 mV (73 mV). These resemblances support our judgment that the only reasonable origin of the present $G(V,x,y)$ is in the superconducting DOS. A careful discussion supporting identification of $G(V)$ with the electronic spectrum, given in Ref. 6, also applies here. Further, the STS $G(V)$ curves have a reasonable resemblance to curve *d*, typical of conventional tunneling results on the same crystals.[15] That true vacuum tunneling achieved at 4.2 K is indicated by the topograph and additional experiments in which the set current (tip height) has been varied. Measurements at varying set current from 1 to 10 nA at 450 mV (decreasing tip height) show the same spectral shapes as in Fig. 5.[22] Coulomb effects seem absent, as neither oscillations in V nor voltage shift with tip height,[23] expected for the "Coulomb staircase,"[23] are seen. The strikingly local variations of $G(V)$ on the scale of 50–100 Å $> \xi_{a,b} \sim 24$ Å (see Fig. 2) are admissible for the superconducting DOS. We believe that these variations are probably due to variations in the metallicity of the BiO surface, reflected in $G(V)$ by the proximity effect.

Superconducting proximity effect (SPE) model

The hypothesis is that curves as in Fig. 5(b) occur where BiO is nonmetallic, and the sampled DOS is that of the CuO_2 system. In this case, the BiO layer remains quite transparent to electrons, compared with the vacuum and SrO barriers, since the conduction-band edge in the BiO is still close to the Fermi level. In the "highly peaked" regions, where we assume the upper BiO layer is metallic, the tunneling DOS samples the superconductivity of this layer, which may change the spectrum to Fig. 5(a) by the nature of the SPE. Here $G(V)$ is determined by the DOS reading in the N layer, as it interacts by SPE with the CuO_2 layers.

A simple SPE model for the N layer has been used to provide the dashed curves in Fig. 5(a), based upon the dashed curve in Fig. 5(b). McMillan's "tunneling model" of an N-I-S proximity bilayer[24] assumes an equal probability of tunneling between each state in S and each state in N, independent of relative momenta. In this simplified model, the energy-dependent gap function in N, $\Delta_N(E)$, is exactly soluble in terms of $\Delta_S(E)$, and the tunneling rate from N to S, Γ_N:

$$\Delta_N(E)=\Gamma_N\Delta_S(E)/[(\Delta^2-E^2)^{1/2}+\Gamma_N]\ , \quad \Gamma_N=\hbar/2\tau_N\ ,$$

with τ_N the residence time in N against tunneling to S. The resulting normalized $G(V)$ is given[24] in the standard way: $G_{S(N)}(V)=\mathrm{Re}[E/(E^2-\Delta_{S(N)}{}^2)^{1/2}]$.

Applying this model entails the fundamental difficulty that neither $G_S(E)$ nor the correct $\Delta_S(E)$ for the HTS CuO_2 layer is known. For lack of a better approach, we have used the BCS $G_S(E)$ and have taken a constant complex value for Δ_S. For this reason, one does not expect to fit the data curves. However, since it is known that HTS does exhibit SPE on simple metals such as Au, we believe that the approach we take is correct in principle for showing the characteristic change in $G(V)$ in the N layer. Presumably better results would be obtained with improved knowledge of G_S and Δ_S.

We have taken $\Delta_S=41+i6$ (meV) for curve *b*, and have modeled curve *a* with the same Δ_S and $\Gamma_N=106$ meV. In both cases an imaginary part (4–7 meV) has arbitrarily been added to E in calculating G to simulate thermal and other broadenings. Although this is a simplified approach which neglects the effect of N on S, the basic physics seems appropriate. The results [dashes, Figs. 5(a) and 5(b)] demonstrate, albeit crudely, the narrowing and heightening effect of the N-side spectrum, as expected in the McMillan tunneling model, here in the strong-coupling limit. The rather strong coupling $\Gamma_N \approx 100$ meV is quite reasonable, and suggests that in the absence of the N layer, tunneling into S from the tip will be limited as usual by the vacuum barrier. This strong inferred coupling internal to the 15.4 Å N-I-S/S-I-N half-cell likely exceeds that between adjacent half-cells, justifying neglect of the rest of the crystal for the purposes of this rough estimate.

In the weak-coupling limit,[24] Γ_N becomes the gap induced in N and corresponds to the *c*-direction tunneling. Smaller tunneling rates (smaller gaps) are predicted for oblique transitions (with an a,b component), a conclusion retained in the clean limit result.[25] It is plausible from this point of view that a gap related to the BiO electrons might appear larger in a *c*-direction measurement than in an a-b-direction measurement such as PES.[2–4]

The highly stepped region does not reveal a superconducting $G(V)$, but a $G(V)$ minimum or a V-shaped $G(V)$. *In situ* cleaved b-c or a-c faces would definitely be expected to reveal superconductivity, e.g., as seen by Mandrus *et al.*[26] However, a highly stepped region resulting from crystal growth, or as cleaving damage (breaking strong bonds) in air ambient, would likely be off stoichiometry, possibly disordered, and nonsuperconducting.[17] This seems consistent with our data. The linear (nonsuperconducting) $G(V)$ curves [Fig. 5(e)] seem to arise more often in locations of steepest $z(x,y)$ slope, including some sites in the grain boundary near $y=350$ Å; these may indicate some tunnel transitions into nonsuperconducting CuO_2 planes, with $\mathbf{k}\|a,b$.

The values of peak position $V_p \approx 40$–50 mV in Fig. 5, and our estimate above of 41 meV for Δ_s, indicate a large gap parameter for 2:2:1:2. This is presumably associated with the *c* direction in the material because of the known peaking of electron barrier transmission for normal incidence. To approximate curves like *a* and *b* in Fig. 5, we estimate that Δ values in the range 36–41 mV, or $2\Delta/kT_c=9.3$–10.6, are required. The present values of V_p exceed those near 35 mV in our conventional junctions,[15] also sampling the *c* direction, and those that show

$G(V)$ disappearing at the correct bulk T_c. A possible origin of the reduced V_p and Δ, preserving T_c, is surface depression of Δ by the grown barrier of the conventional junctions, important[27] in view of the very short $\xi_c \sim 1$ Å and extrapolation lengths. The present vacuum tunneling data should be a better measure of Δ, since the surface is free and has been only briefly exposed to air. The present gap estimates also exceed $\Delta_{a,b} \approx 25$ meV.[24,26] At face value an anisotropic Δ_k enlarged along c is implied. This is probably consistent with an "isotropic" 3D Δ_k resulting from interlayer models;[28,29] the possibility of depressed values of $\Delta_{a,b}$ may also exist.

All of these curves in Fig. 5 have "states in the gap" at the level $G(0)=0.15-0.2$, and $G(V)$ rising as a low power of V. Such states may come from the proximity effect,[9,24] or from models with a node in the gap function, e.g., in d-wave pairing,[30] or via interlayer pairing;[29] and possibly the repulsive pairing model[31] could lead to this appearance near $V=0$. The latter approaches[30,31] probably would not explain the "high-peaks" shape of Fig. 5(a), unless incorporated into a proximity effect picture. The "highly peaked" shape is predicted by Ref. 24, although functional forms to compare to the data are unavailable.

To summarize, we have mapped at 5 Å resolution the DOS for tunneling into the a-b plane of 2:2:1:2. Analysis of 10^4 $G(V)$ spectra shows a large gap Δ_c in the range 36–41 meV ($2\Delta/kT_c = 9.3-10.6$) on the a-b plane, with $\sim 20\%$ variations on as small a scale as ~ 50 Å, near certain sites. The superconducting $G(V)$ disappears in a highly stepped defective region and in localized regions near a grain boundary, leaving a broad minimum or V-shaped $G(V)$. With some notable exceptions, which we associate with depressed superconductivity in highly stepped regions, changes in the characteristic shape of $G(V)$, as in a and b of Fig. 5, seem to correlate with enhanced peaks in apparent z. We interpret such "electronically elevated" areas, also seen in Refs. 7 and 13, as regions of enhanced $N(0)$ and metallicity in the surface BiO layer, reflected in the superconducting DOS by the superconducting proximity effect. However, we cannot entirely rule out possible effects arising from spatial variation of the work function. The spectroscopy results confirm a recent STM report[5] of a large gap in BSCCO (2:2:1:2) along the c direction. An increase in the estimated Δ_c values, 36–41 meV, over those obtained from conventional Pb-I-BSCCO junctions,[15] is attributed to surface lowering[27] of the order parameter by the grown barrier in the latter case.

We thank D. B. Mitzi for advice on crystal growth, and G. B. Arnold, R. A. Klemm, S. H. Liu, and M. Onellion for discussions of the results. This work was supported by the U.S. Department of Energy, Office of Basic Energy Sciences, under Grant No. DE-EG02-87ER45301.

[1]W. C. Lee, J. H. Cho, and D. C. Johnston, Phys. Rev. B **43**, 457 (1991).
[2]B. O. Wells *et al.*, Phys. Rev. Lett. **65**, 3056 (1990).
[3]D. S. Dessau *et al.*, Phys. Rev. Lett. **66**, 2160 (1991).
[4]Y. Hwu *et al.*, Phys. Rev. Lett. **67**, 2573 (1991).
[5]T. Hasegawa, M. Nantoh, and K. Kitazawa, Jpn. J. Appl. Phys. **30**, L276 (1991).
[6]J. X. Liu *et al.*, Phys. Rev. Lett. **67**, 2195 (1991).
[7]C. Wang, B. Giambattista, C. G. Slough, R. V. Coleman, and M. A. Subramanian, Phys. Rev. B **42**, 8890 (1990).
[8]Z. X. Shen *et al.*, Phys. Rev. B **44**, 12 098 (1991).
[9]M. Tachiki, S. Takahashi, F. Steglich, and H. Adrian, Z. Phys. B **80**, 161 (1990).
[10]E. Braun *et al.*, Z. Phys. B **84**, 333 (1991).
[11]J. D. Jorgensen, Phys. Today **44**(6), 34 (1991).
[12]A point-contact mode STM gap mapping on $YBa_2Cu_3O_{9-y}$ at 1000 Å resolution, in which the tip punctured the surface on each measurement, was reported by A. P. Volodin and M. S. Khaikin, Pis'ma Zh. Eksp. Teor. Fiz. **13**, 1034 (1987) [JETP Lett. **13**, 588 (1987)].
[13]We take ϕ as constant, although we cannot strictly rule out spatial variations, especially small variations as a consequence of local changes in n and E_F. In Ref. 7, apparent z peaks (very similar to ours) are attributed to "variation in local electronic structure in layers below the surface" [which we model as $N_{\mathrm{BiO}}(O,x,y)$]; the measured ϕ values are presented as being independent x,y.
[14]D. B. Mitzi *et al.*, Phys. Rev. B **41**, 6564 (1990).
[15]E. L. Wolf, H. J. Tao, and B. Susla, Solid State Commun. **77**, 519 (1991); H. J. Tao, A. Chang, F. Lu, and E. L. Wolf, Phys. Rev. B **45**, 20 622 (1992).
[16]M. D. Kirk *et al.*, Appl. Phys. Lett. **52**, 2071 (1988).
[17]T. Komeda, G. D. Waddill, P. J. Benning, and J. H. Weaver, Phys. Rev. B **43**, 8713 (1991).
[18]The grain boundary is best seen in Fig. 1(d), or in plots (e.g., Fig. 3, solid curve) of z vs y near $y=350$ Å, $0<x<400$ Å. The saturation of the gray scale (white region) and some x,y smoothing specific to Fig. 1(a) have obscured the grain boundary. Corrugations are on the scale of 5 Å in the plateau regions, slightly larger than 4 Å reported (Ref. 16) for the b-axis superlattice, which is not clearly resolved here. We cannot rule out that some of the roughness seen in Figs. 1(a) and 1(d) arises from variations in local work function, but we believe that variation of $N(0,x,y)$ is the more likely origin. A correlation analysis of $z(x,y)$ in the 350×200 Å^2 region at $x=0,y=0$ [A. Chang, Yu. M. Ivanchenko, Z. Y. Rong, and E. L. Wolf, Surf. Sci. Lett. **274**, 504 (1992)] reveals the known 27.5-Å superstructure (Ref. 16), with the b axis at $\pm57°$ with respect to the x axis in Figs. 1(a), 1(b), and 1(d). Several clear examples of 16-Å (half-cell) steps (Ref. 16) of finite length can be seen in line plots of z in the lower plateau of Fig. 1. The origin of these finite length steps will be described elsewhere [Yu. M. Ivanchenko, A. Chang, Z. Y. Rong, and E. L. Wolf (unpublished)].
[19]X. L. Wu, Y. L. Wang, Z. Zhang, and C. M. Lieber, Phys. Rev. B **43**, 8729 (1991).
[20]Since the background conductance rises toward positive bias, normalizing by $G(168$ mV) artificially depresses these normalized values by about 13%. Thus the G_{Peak} values in Fig. 3 should be multiplied by about 1.13.

[21]The variations in stoichiometry are likely present in the crystals (see Refs. 7, 11, and 19) although effects of the brief air exposure cannot be entirely excluded. The measured $G(V)$ is expected to be affected by variations in the sample stoichiometry primarily via their effect on the electronic spectrum of the superconducting state at the location of the final state in the tunneling transition. When the BiO layer is insulating, such final states are presumably in the CuO_2 layer; when the BiO layer is metallic, the final states are in the BiO layer. The state of superconductivity in the BiO layer may depend on its $N(0)$, the tunnel barrier between it and the CuO_2 layer, and the state of superconductivity in the CuO_2 layer. All of these can be influenced by local stoichiometry.

[22]A different possible origin of the "highly peaked" spectra arises if ϕ spatially varies, causing the tip-sample spacing s to vary [at constant I and $N(0)$]. This might bring in "peaking" of spectra observed as a function of s, reported in Fig. 4 of Ref. 5. We cannot strictly rule this out, but we do not believe it is important here; see Ref. 13 and the text in connection with invariance of our spectra with varying set current. The "peaking" effects of Ref. 5 presumably occur at smaller s than employed here.

[23]Z. Y. Rong, A. Chang, L. F. Cohen, and E. L. Wolf, Bull. Am. Phys. Soc. **36**, 873 (1991); IEEE Trans. MAG **28**, 67 (1992).

[24]W. L. McMillan, Phys. Rev. **175**, 537 (1968).

[25]P. G. de Gennes and D. Saint-James, Phys. Lett. **4**, 151 (1963).

[26]D. Mandrus, L. Forro, D. Koller, and L. Mihaly, Nature (London) **351**, 460 (1991).

[27]G. Deutscher and K. A. Müller, Phys. Rev. Lett. **59**, 1745 (1987).

[28]P. W. Anderson, Phys. Rev. B **42**, 2624 (1990).

[29]R. A. Klemm and S. H. Liu, Phys. Rev. B **44**, 7526 (1991); S. H. Liu and R. A. Klemm, *ibid.* **45**, 415 (1992).

[30]C. T. Rieck, D. Fay, and L. Tewordt, Phys. Rev. B **41**, 7289 (1990).

[31]F. Mila and E. Abrahams, Phys. Rev. Lett. **67**, 2379 (1991).

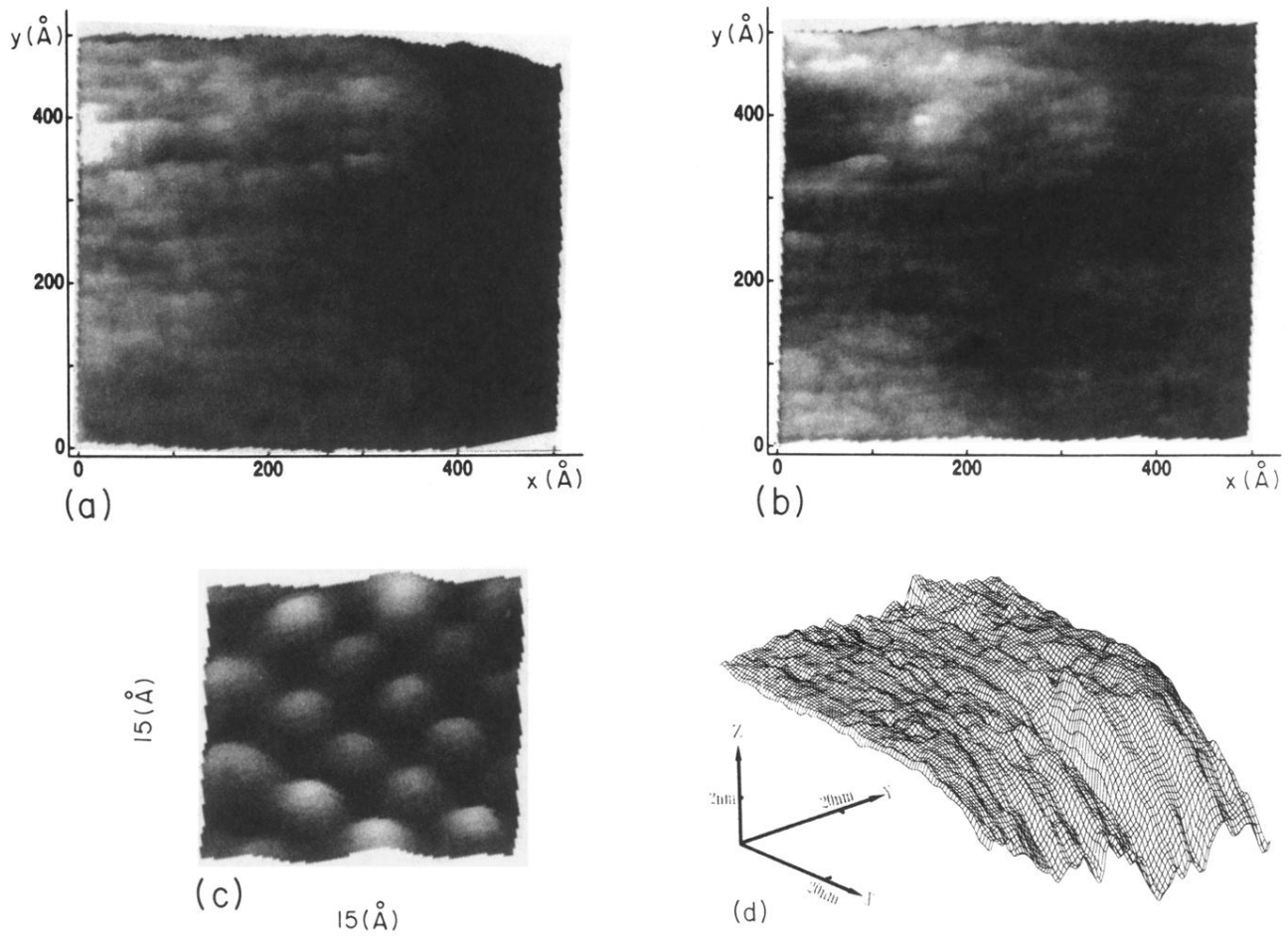

FIG. 1. (a) Topograph at 4.2 K of 500×500 Å^2 region at 5 Å spacing; 1 nA at 200 mV tip bias. Gray scale range [$z(x,y)$ variation] is 40 Å; in a highly stepped region (right), z falls a further ≈100 Å, off scale. (b) Gray scale image of maximum $G_{\text{Peak}}(x,y)/G(168$ mV) of $G(V)$, $-168<V<168$ mV (tip bias), acquired in 10^4 pixels. White areas exhibit $G_{\text{Peak}}/G(168$ mV) up to ~1.9. (c) Topograph of 15×15 Å^2 square of similar BSCCO crystal *in situ* cleaved and imaged using a more stable STM at 1.2×10^{-9} Torr, using etched Pt-Ir tip at -290 mV and 1.2 nA current. (d) Perspective view of the same data as in (a), calibration shown, which more clearly reveals details near the joining of the two plateau regions, $0<x<30$ Å, $350\text{Å}<y<400$ Å.

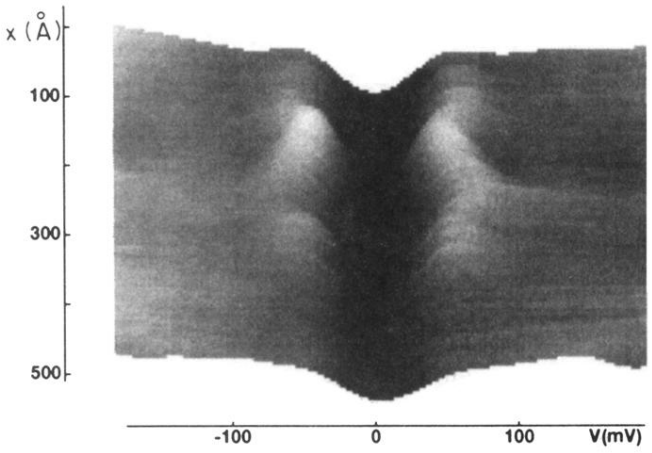

FIG. 2. Local variation of $G(v,x,y)/G(168\ \text{mV})_{av}$ (gray scale range 0.12–1.36). Curves taken at 5-Å intervals for $0 < x < 500$ Å (top to bottom), averaging $G(V)$ over $375 < y < 400$ Å (six rows).